

# Using the IEC standard to describe low-background detectors - what may one expect?

Ronald M. Keyser and Sanford Wagner  
EG&G ORTEC  
100 Midland Road  
Oak Ridge, TN USA 37830

Presented at the 1998 Winter Meeting of the American Nuclear Society, Nov 15, 1998, Washington, DC

## Summary

Many measurements for environmental levels of the radioactive content require that the gamma-ray detector be “low background”, that is, free of any radioactive content. This is, of course, not possible, but the radioactivity in the detector must be reduced to as low a value as possible. The description or specification of the background spectrum necessary to achieve the desired results is needed.

At present, many different ways are used to describe the background spectrum for low-background detectors. In this context, the background spectrum is all counts in the spectrum that do not come from the sample being measured. This background may come from radioactive content in the materials used to make the detector, from the materials used to make the shield, or from activation of the detector and shield materials by cosmic rays.

Some of the ways to describe the background relate to measurement performance and some do not. For example, specifying the background in “counts per channel per unit time” gives different results for different ADC conversion gains (total number of channels) and for different amplifier gains (total energy range). Also, specifying the peak areas (full energy peaks) for identifiable peaks in the spectrum gives variable results unless the calculation for peak area is defined and it must be normalized for detector size. Another ambiguous specification is the specification of the maximum activity for a particular isotope. The activity depends on the efficiency value, which is detector/sample geometry dependent.

The new IEC standard<sup>1</sup> for describing the background makes the specification of the background in an HPGe detector simple, unambiguous and related to how the detector will be used. Users and manufacturers will finally be speaking the same language on this subject. For example, the non-peak background is given in “counts per kilovolt per 1000 seconds” by the following:

$$B(E) = \frac{1000}{T_L} \times \frac{G}{5 \times F(E) + 1} \times \sum_{i=j-2.5F(E)}^{j+2.5F(E)} C_i \quad (1)$$

Where:

$B(E)$	=	average background per keV per 1000 sec at energy $E$
$G$	=	the conversion factor from channels to energy, in channels/keV
$F(E)$	=	the resolution (in channels) of the detector at energy $E$
$C_i$	=	the channel contents of channel $i$
$j$	=	the channel corresponding to energy $E$
$T_L$	=	the livetime in seconds

---

<sup>1</sup> IEC 45/430/CD, Nuclear Instrumentation - Spectrometry - Test methods for spectrum background determination in HPGe nuclear spectrometry.

This value is independent of any hardware setting.

The peak area is defined by:

$$A_{NP}(E) = \frac{1000}{T_l} \times \left[ \sum_{i=j-1.5F(E)}^{j+1.5F(E)} C_i - \sum_{i=j-3.0F(E)-1}^{j-1.5F(E)-1} C_i - \sum_{i=j+1.5F(E)+1}^{j+3.0F(E)+1} C_i \right] \quad (2)$$

Where  $A_{NP}(E)$  is the net peak area corresponding to energy  $E$ ,  
 $j$  is the channel number corresponding to energy  $E$ .

Since this standard extends the specification of the performance of an HPGe detector, there is little history available for comparison and thus no means of determining a “good” value. To develop a history, the background spectrum for 400 low-background HPGe ORTEC detectors were all counted in similar low-background shields. These detectors were in a variety of mechanical cryostat and endcap configurations. The continuum background will be presented as a function of energy and detector size/configuration. The peak area for the peak energies listed in the standard will be presented as a function of detector size and configuration. The results presented will give practical guidance for obtaining the most appropriate low-background detector for a specific measurement problem.

## Introduction

The increase in concern for the environment and the decommissioning of many facilities where radioactive materials were used has increased the need for and use of low-background, high-purity-germanium detector systems. In the past, there has not been a uniform way for specifying the performance of these systems. Many different details were described or prescribed in an attempt to predict the usability of the detector system for detecting low levels of radioisotopes. None of these specifications proved to be a reliable way to specify and purchase a system. In 1996, work was started in the International Electrotechnical Commission and IEEE working groups for nuclear standards. The result of that work is an IEEE standard and a proposed IEC standard for specifying the background of germanium detectors.

These standards define terms related to the background and describe how to calculate values for background in a way that can be reproduced in any situation. What is not described in these standards is particular values that can be obtained for various detectors.

The “background” is defined to be the spectrum in the detector-shield with no source present, as shown in Fig. 2. The radiations causing this background come from the detector materials, the shield materials and cosmic ray interactions with the detector, detector materials and the shield materials.

The shield (Fig. 3) used to measure the background of EG&G ORTEC low-background detectors consists of an inner layer of 5 cm OFHC copper with an outer layer of 15 cm of low-activity lead. For HJ type cryostats, the bottom of the detector is covered with a 1 cm lead bowl with a 1 mm copper liner. The floor below the shield is covered by 10 cm of lead. For cryostats where the detector is “down-looking”, another shield with the opening at 45° from the vertical is used.

The background is affected by many factors, including:

1. Geographic location of the measurement
2. Shielding material(s), thickness(es) and geometry (including detector position)
3. Date and time of the measurement

4. Weather conditions at time of measurement
5. Duration of measurement
6. Airbourne activity

Thus, any results derived from the use of these methods should have all of the measurement details described.

The background can be described as consisting of two parts: the full-energy peaks of nuclide specific gamma rays and the smooth or non-peak background. Both of these are important. The presence of full energy peaks in the spectrum can mask the presence of these nuclides in the sample. The presence of the non-peak background is the major factor in the attainable MDA.

The formula in Eq. 2 defines how to calculate the net peak area rate. This uses a peak width of 3 times the FWHM for the detector for the peak region with the same width for the underlying continuum split above and below the peak region. The peaks in low-background spectra are contained in the 3 FWHM width. Fig. 4 shows this for a specific peak. The result is specified as a count rate so that it is independent of the counting time. It is multiplied by 1000 (i.e., counts per 1000 seconds) so that the values obtained are expected to be between 10 and 0.1. An implicit assumption is that the FWHM is more than one channel. Specifically not used is any conversion to activity, which requires an efficiency and a statement of the nuclide.

Fig. 5 shows the construction of a typical detector. Note the differences in material thickness for the various gamma-ray paths to the crystal. The background radiations come from all directions and not confined to the geometry of any efficiency calibration. This means that the background peak areas cannot be expressed in activity in the background, but do contribute to the activity of a given sample.

The formula in Eq. 1 defines how to calculate the background in any region of the spectrum. This uses a region width of 5 times the FWHM for the detector. This width will smooth out the variation from channel to channel in the spectrum, as shown in Fig. 6. The result is given as counts/keV/second. This removes any dependence on the number of channels in the spectrum, the amplifier gain, and the counting time.

Just stating the peak and background count rates is not enough information to describe the detector, so the following results are shown as a function of the detector crystal diameter, length and volume. These results are for all types of detector cryostats, which gives some variation in the values.

Fig. 7 shows the wide range of detector sizes in the study. Approximately 400 detectors are shown here.

### **Example peak areas**

The 2614 peak is due to Tl-208 (Thorium natural decay series). Fig. 8 shows the net peak count rate of the 2614-keV peak vs detector volume. There is a wide variation in the peak area shown. The overall trend is increasing from about 0.5 to 2.5 counts per 1000 sec per keV from smallest to largest volume. The volume increases from about 100 cc to 800 cc. This reflects the increase of high energy efficiency with increasing detector size.

Fig. 9 shows the net peak count rate of the 2614-keV peak vs detector diameter. This shows the same high scatter with detector diameter as for detector size. The peak count rate also increases with increasing diameter.

Fig. 10 shows the net peak count rate of the 2614-keV peak vs detector length. This shows the

same high scatter with detector length as for detector size. The peak count rate also increases with increasing length.

Fig. 11 shows the net peak count rate of the 1460 keV peak vs detector volume. There is a wide variation in the peak count rate shown. The overall trend is increasing from about 0.3 to 0.4 counts per 1000 sec per keV from smallest to largest volume. This is much smaller than the increase in detector volume (1:8). This reflects the increase of high energy efficiency with increasing detector size, but also shows that the 1460 keV does not penetrate enough to utilize the increase size.

Fig. 12 shows the net peak count rate of the 1460 keV peak vs detector diameter. This shows the same high scatter with detector diameter as for detector size. The peak count rate also increases with increasing diameter.

Fig. 13 shows the net peak count rate of the 1460 keV peak vs detector length. This shows the same high scatter with detector length as for detector size. The peak count rate also increases with increasing length.

Fig. 14 shows the net peak count rate of the 185 keV peak vs detector volume. Again, there is a wide variation in the peak area shown. The overall trend is increasing from about 0.25 to 0.65 counts per 1000 sec per keV from smallest to largest volume. For this low energy, the increase is likely due to the increase in surface area of the crystal. However, the increase is not as large as the increase in the surface area or the volume.

Fig. 15 shows the net peak count rate of the 185 keV peak vs detector diameter. This shows the same high scatter with detector diameter as for detector size. The peak count rate also increases with increasing diameter.

Fig. 16 shows the net peak count rate of the 185 keV peak vs detector length. This shows the same high scatter with detector length as for detector size. The peak count rate also increases with increasing length.

## **Background Levels**

The energy regions of 2500, 550 and 100 keV were chosen to be representative of the important energy regions in the background for most applications. The following figures show the background counts/keV/1000 seconds plotted against detector volume, diameter and volume.

Fig. 17 shows the background levels at 2500, 550 and 100 keV vs detector volume. Fig. 18 shows the background levels at 2500, 550 and 100 keV vs detector diameter. Fig. 19 shows the background levels at 2500, 550 and 100 keV vs detector length. Note that the background increases slightly with increased detector size (volume, diameter, or length). The effects of this increase on analytical results are discussed below in the section on Relative Minimum Detectable Activity ( $MDA_R$ ).

## **Relative Minimum Detectable Activity**

Earlier, it was shown that the background increases with increasing detector size, whether that be diameter, length or volume. To determine the effect of this increase in background, the relative figure of merit and the related value, relative Minimum Detectable Activity can be use. Both of there are related to the efficiency and to the background (or null sample) spectrum. The  $MDA_R$  is proportional to the square root of the background area divided by the efficiency at the specified energy, as shown in Eq. 3.

$$MDA_R = \frac{\sqrt{R(E_1)B(E_1)}}{\epsilon(E_1)} \quad (3)$$

Where:  $R(E_1)$  = Resolution at energy  $E_1$   
 $B(E_1)$  = Total background at energy  $E_1$   
 $\epsilon(E_1)$  = Efficiency at energy  $E_1$

Using the background areas calculated here and the efficiencies determined in the following paper, the  $MDA_R$  can be calculated for the different geometries and different crystal sizes. The resolution is assumed to be the same for all detectors. Fig. 20 shows the background for 75 to 85 mm diameter detectors as a function of detector length. Fig. 21 shows the background for  $80 \pm 2$  mm as a function of detector length. The following figures show the  $MDA_R$  for a series of detectors with diameter of  $80 \text{ mm} \pm 2$  mm and lengths of from 58 mm to 101 mm. The difference in length is almost a factor of 2.

Fig. 22 shows the  $MDA_R$  at 150 keV for different geometries. Fig. 23 shows the  $MDA_R$  at 550 keV for different geometries. Fig. 24 shows the  $MDA_R$  at 2500 keV for different geometries. These figures show that the  $MDA_R$  generally decreases with increasing detector size for all source geometries and all energies. Which indicates that the increase in efficiency is more important than the increase in background with increasing detector size. The notable exception is the 2-liter Marinelli beaker geometry, where the length of the detector is important factor in the efficiency value.

## Conclusion

The calculation of the peak areas and background regions for 400 detectors has shown that the methods and formulas given in the IEEE and IEC standards can be used to calculate meaningful results. These results can be used to predict detector performance for many applications.

Since these detectors were manufactured to be low background (i.e., minimal contribution to the background from the detector materials), these spectra represent the gamma rays in the shield due to the shield materials and the surrounding materials as well as the cosmic ray interactions with the shield and detector. Nonetheless, the shield and detector arrangement are much like the average system used for environmental monitoring.



IEC/TC or SC: TC 45	Project number 61976 Ed. 1.0	
Title: Nuclear Instrumentation	Date of circulation 1998-01-23	Closing date for comments 1998-04-30
Also of interest to the following committees	Supersedes document 45/407/CD and 45/420/CC	
Horizontal functions concerned: <input type="checkbox"/> Safety <input type="checkbox"/> EMC <input type="checkbox"/> Environment <input type="checkbox"/> Quality assurance		
Secretary: Mr. Y.P. Seldiakov		THIS DOCUMENT IS STILL UNDER STUDY AND SUBJECT TO CHANGE. IT SHOULD NOT BE USED FOR REFERENCE PURPOSES.  RECIPIENTS OF THIS DOCUMENT ARE INVITED TO SUBMIT, WITH THEIR COMMENTS, NOTIFICATION OF ANY RELEVANT PATENT RIGHTS OF WHICH THEY ARE AWARE AND TO PROVIDE SUPPORTING DOCUMENTATION.

Title:  
Nuclear Instrumentation. Spectrometry. Test methods for spectrum background determination in HPGe nuclear spectrometry

(Titre) :

Introductory note

This document is submitted to the National Committees for comments in accordance with decision taken at the TC 45 meeting in Ischia (Italy) in September 1997, and the discussions of WG 10. The previous draft, 45/407/CD, was discussed in Ischia, and the modifications that have resulted in this draft were reviewed by WG 10 members.

The comments on the previous draft are given in the compilation of comments 45/420/CC.

Figure 1

P20584ab  
P20584A GEM-50195-S LB-SV

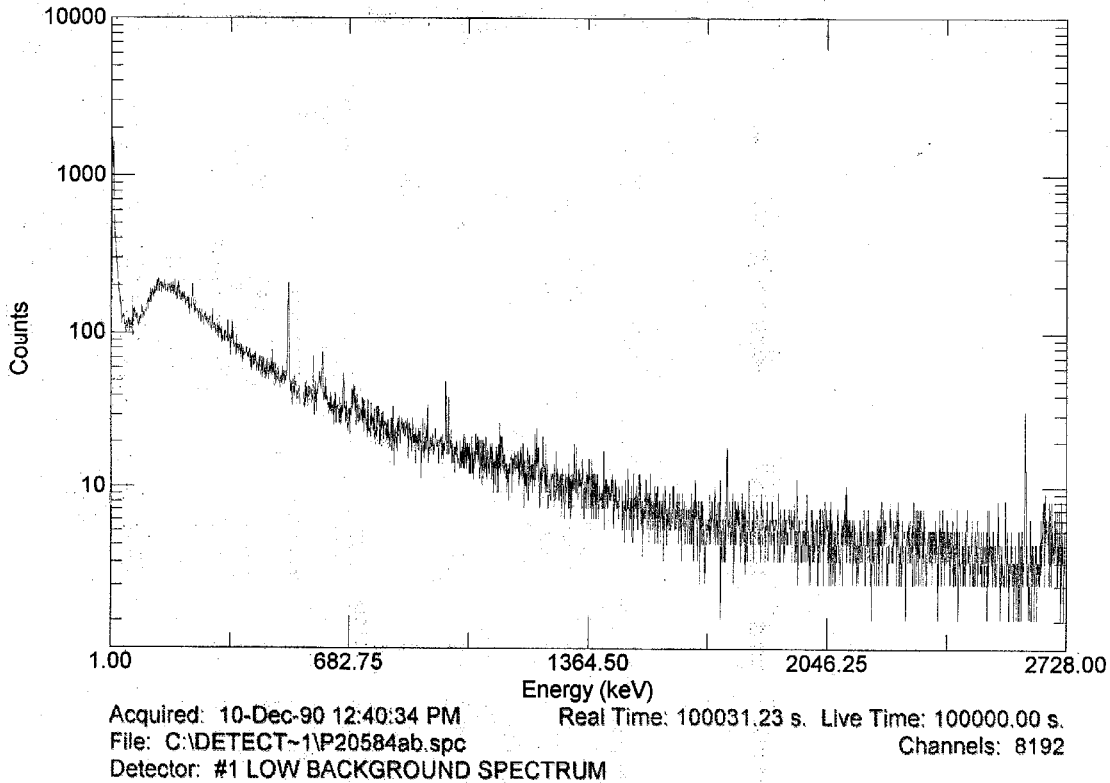


Figure 2

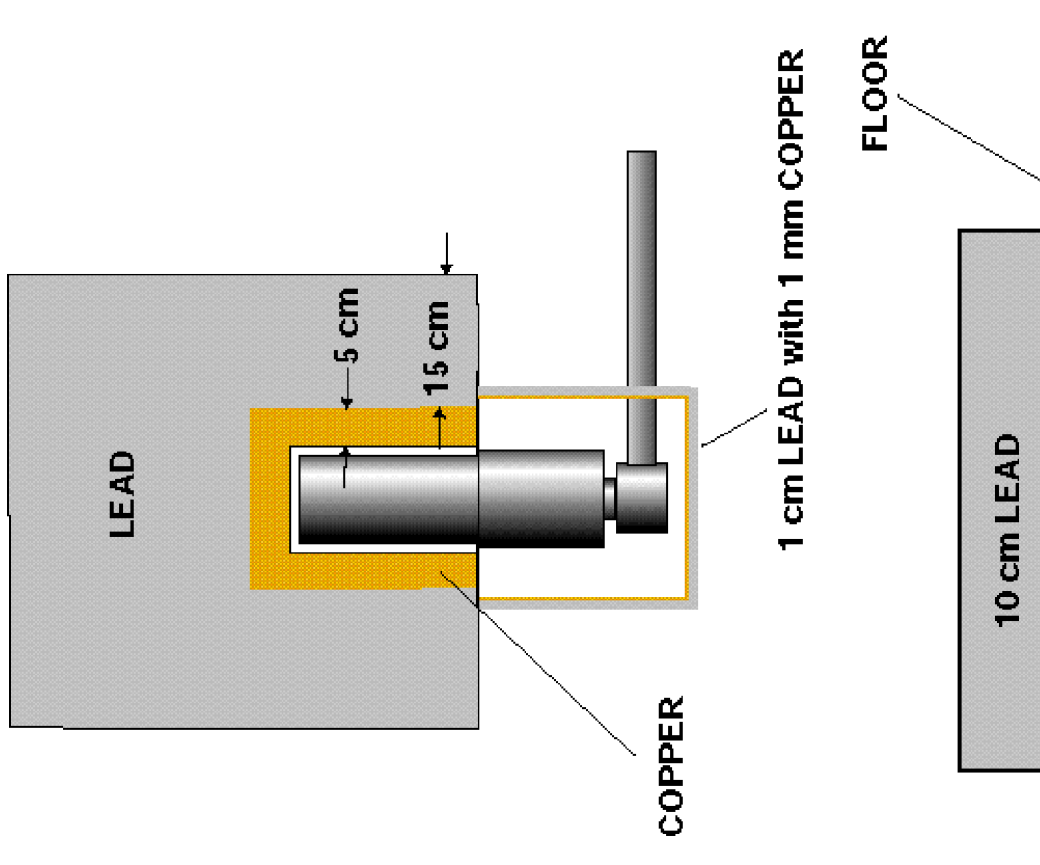


Figure 3

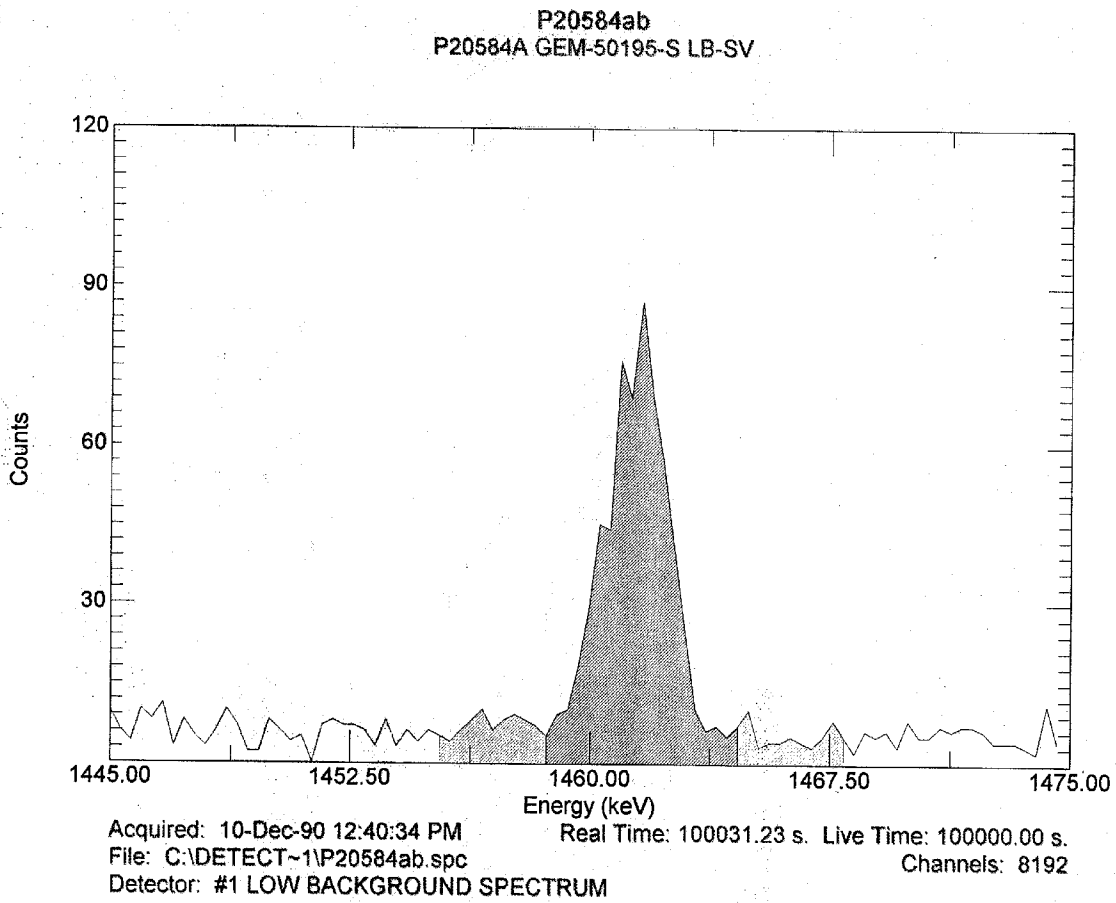


Figure 4

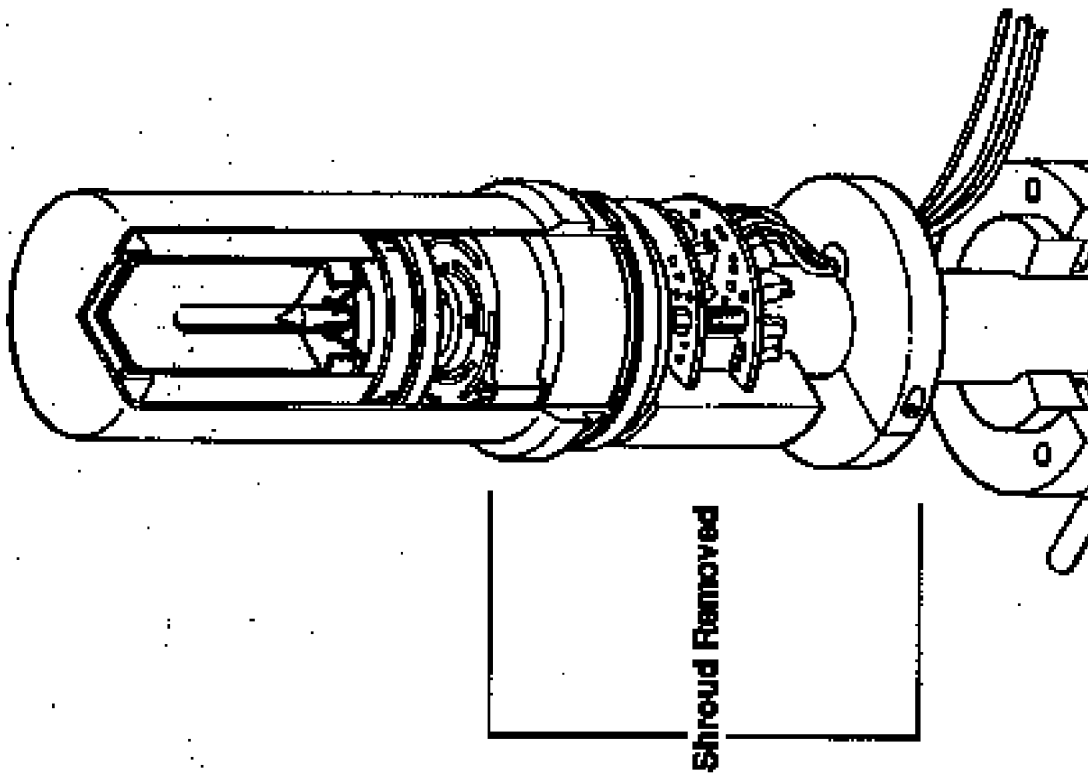


Figure 5

P20584ab  
P20584A GEM-50195-S LB-SV

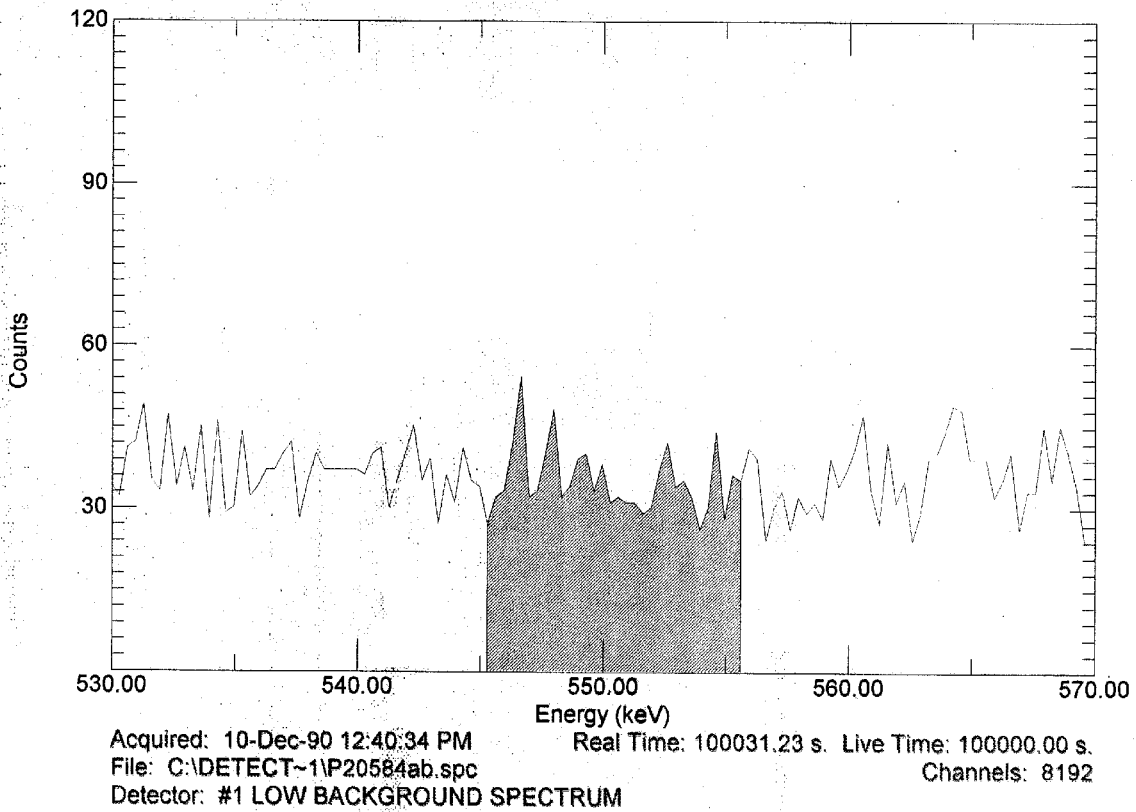


Figure 6

Detectors Studied by Size  
(Total of 400 Detectors)

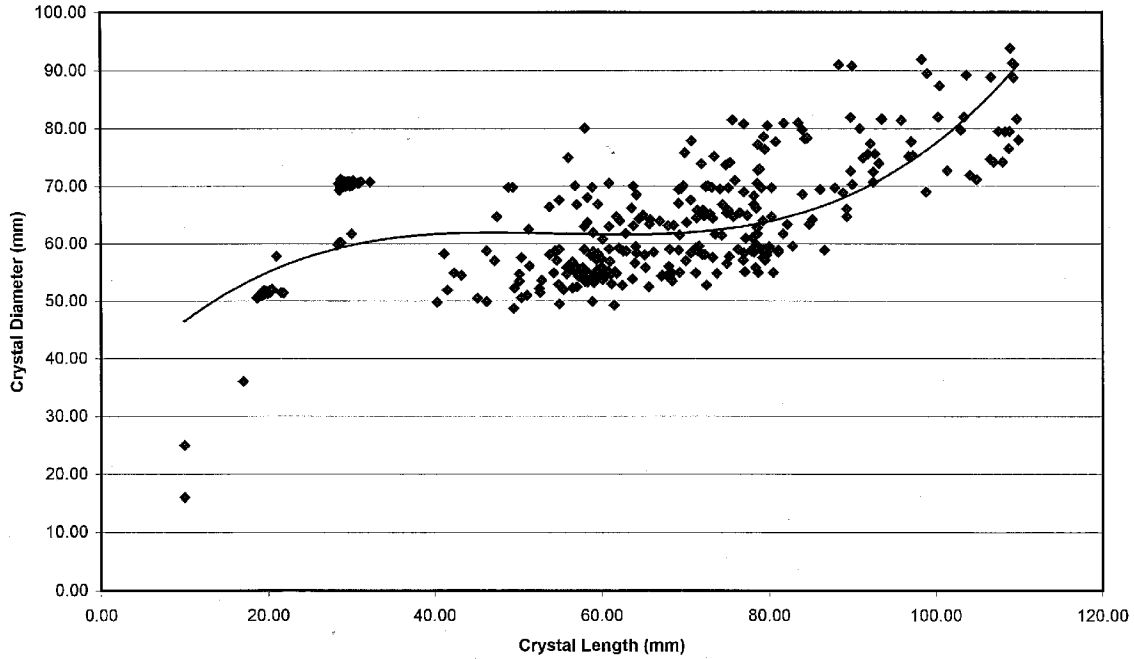


Figure 7

Net Peak Count Rate vs Volume at 2614 keV

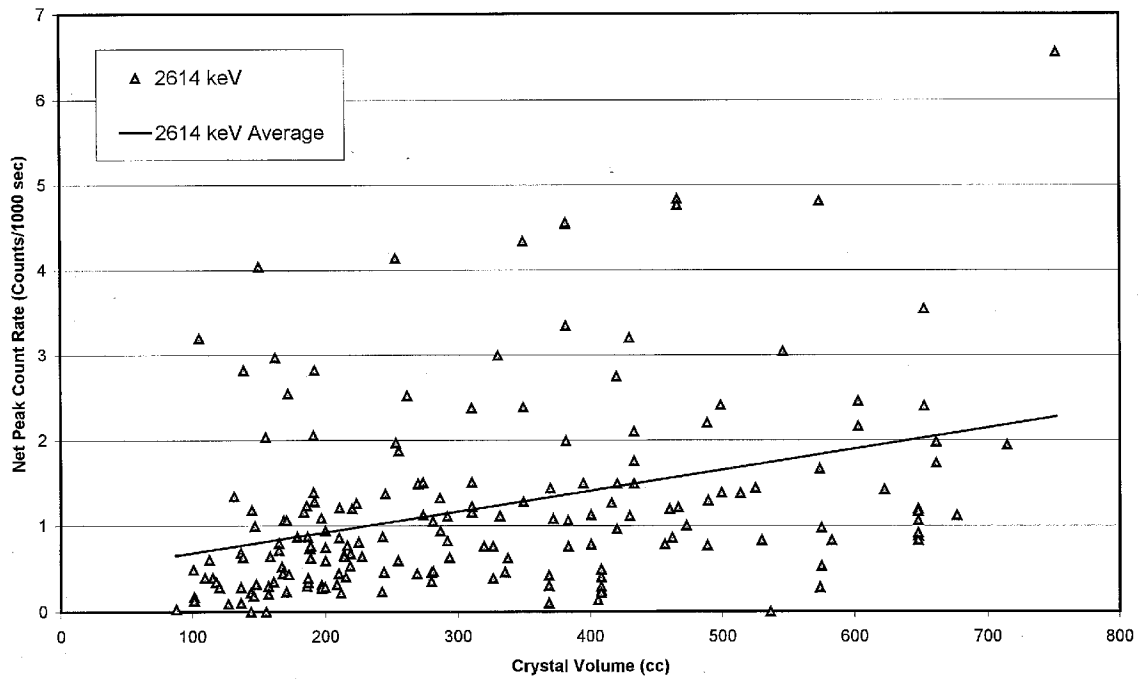


Figure 8

Net Peak Count Rate vs Diameter

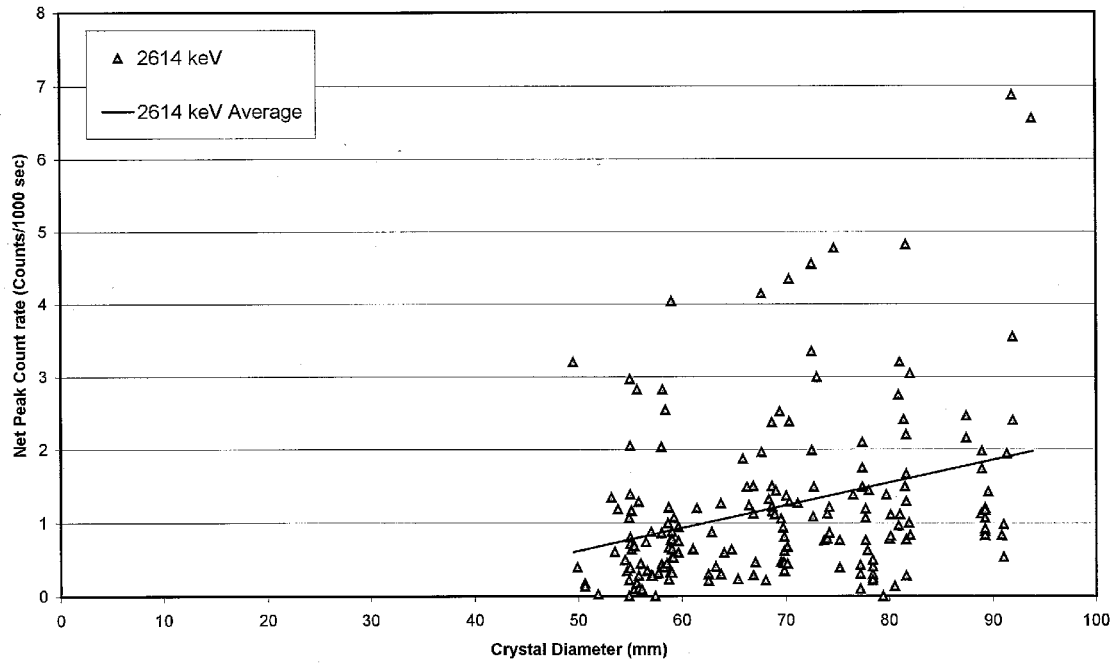


Figure 9

Net Peak Count Rate vs Length at 2614 keV

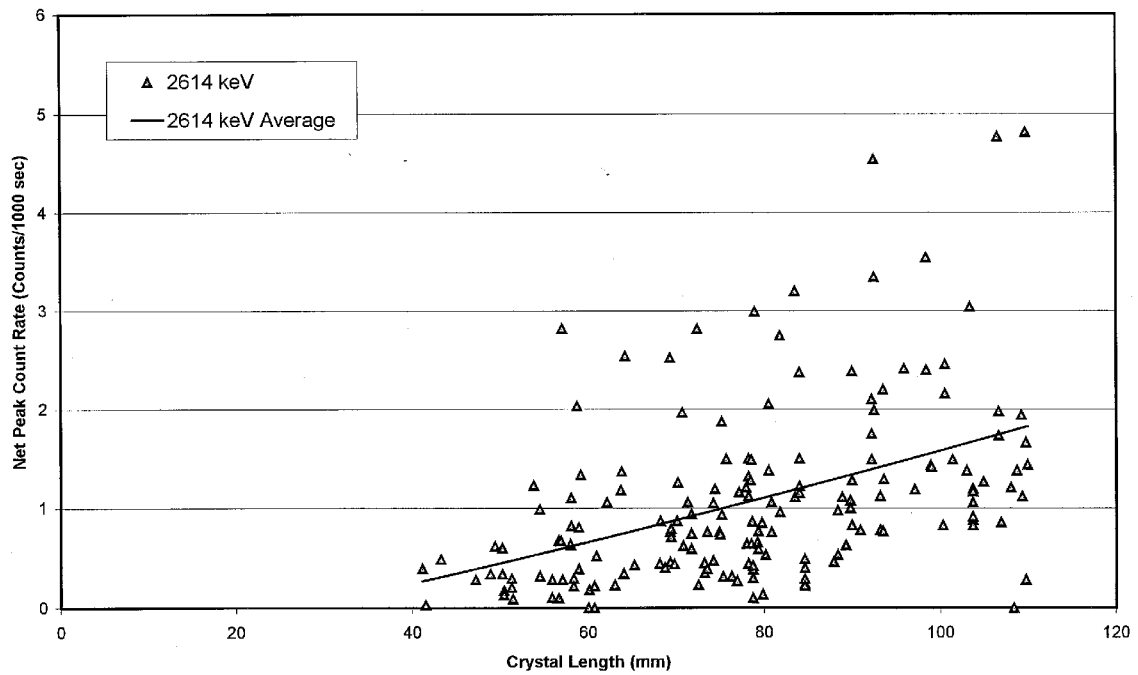


Figure 10

Net Peak Count Rate vs Volume at 1460 keV

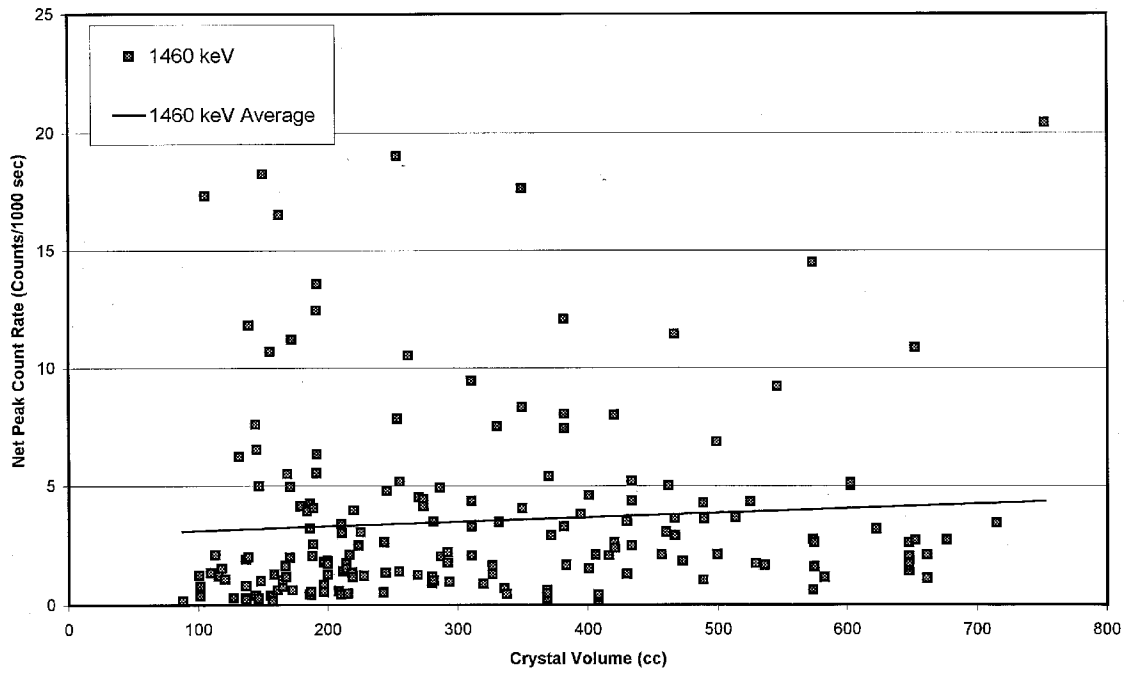


Figure 11

Net Peak Count Rate vs Diameter

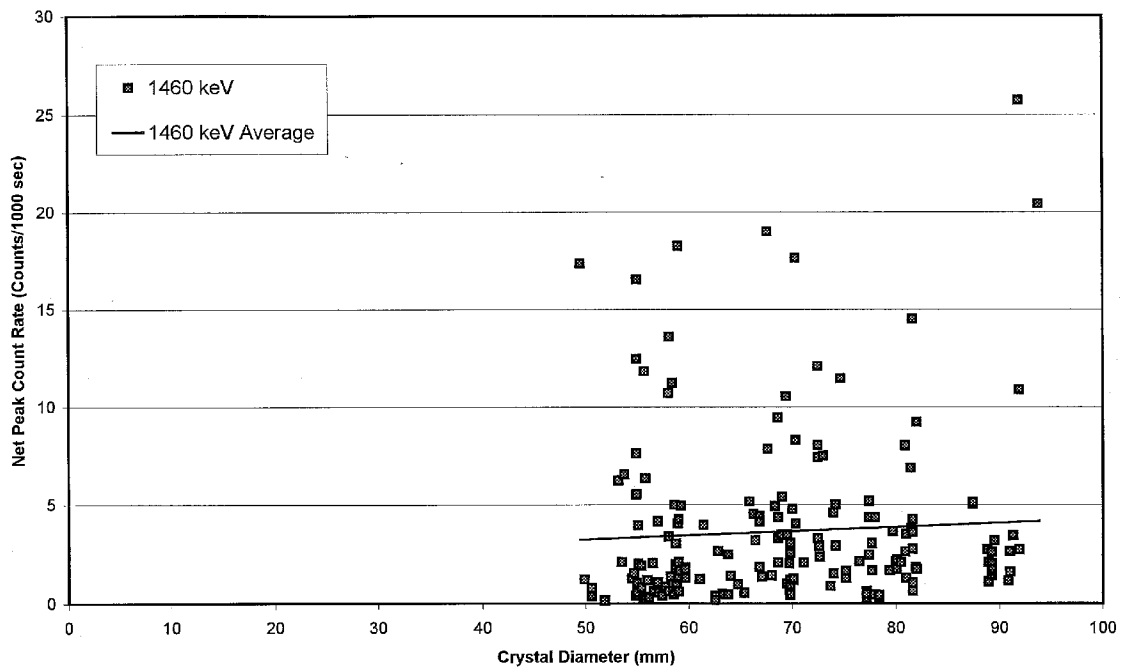


Figure 12

Net Peak Count Rate vs Length at 1460 keV

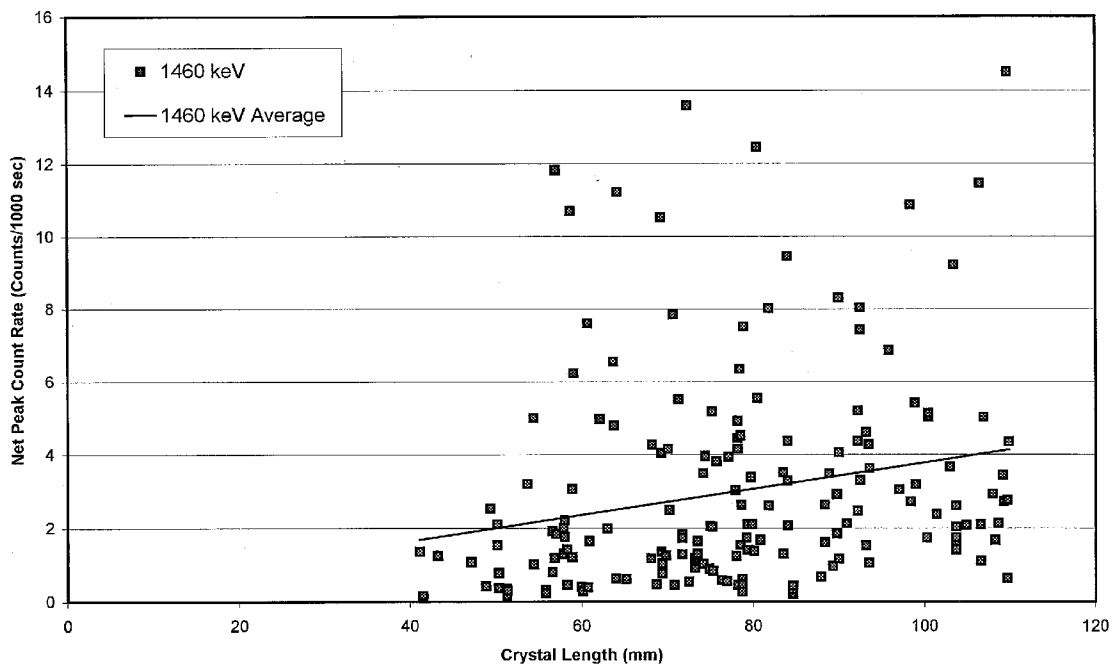


Figure 13

Net Peak Count Rate vs Volume at 185 keV

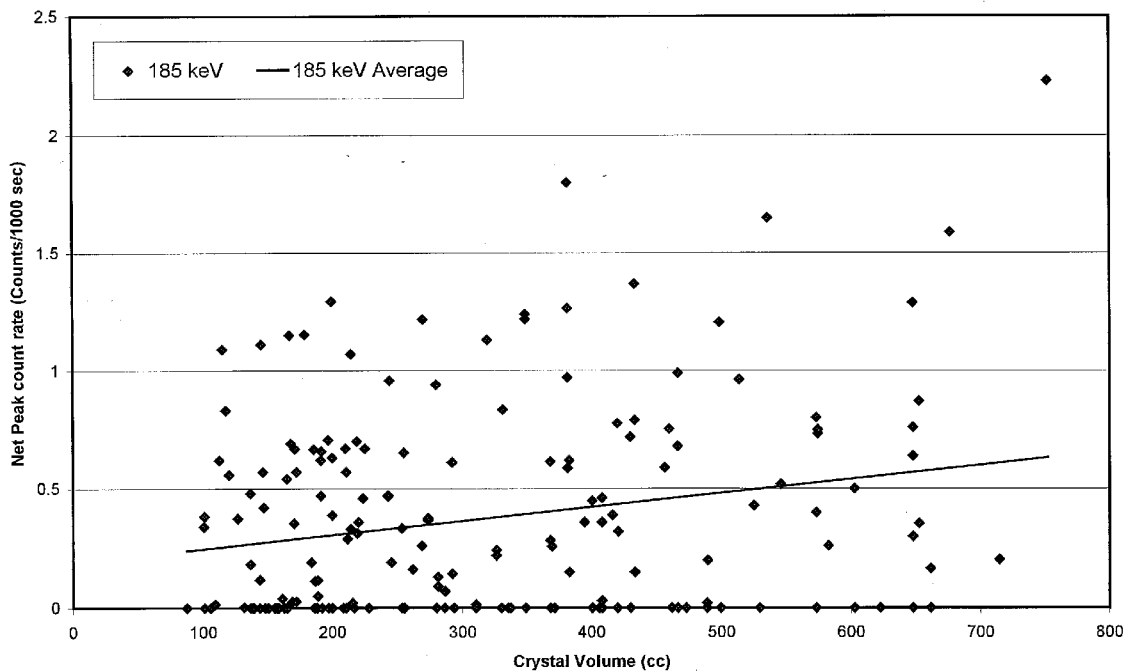


Figure 14

Net Peak Count Rate at 185 keV vs Diameter

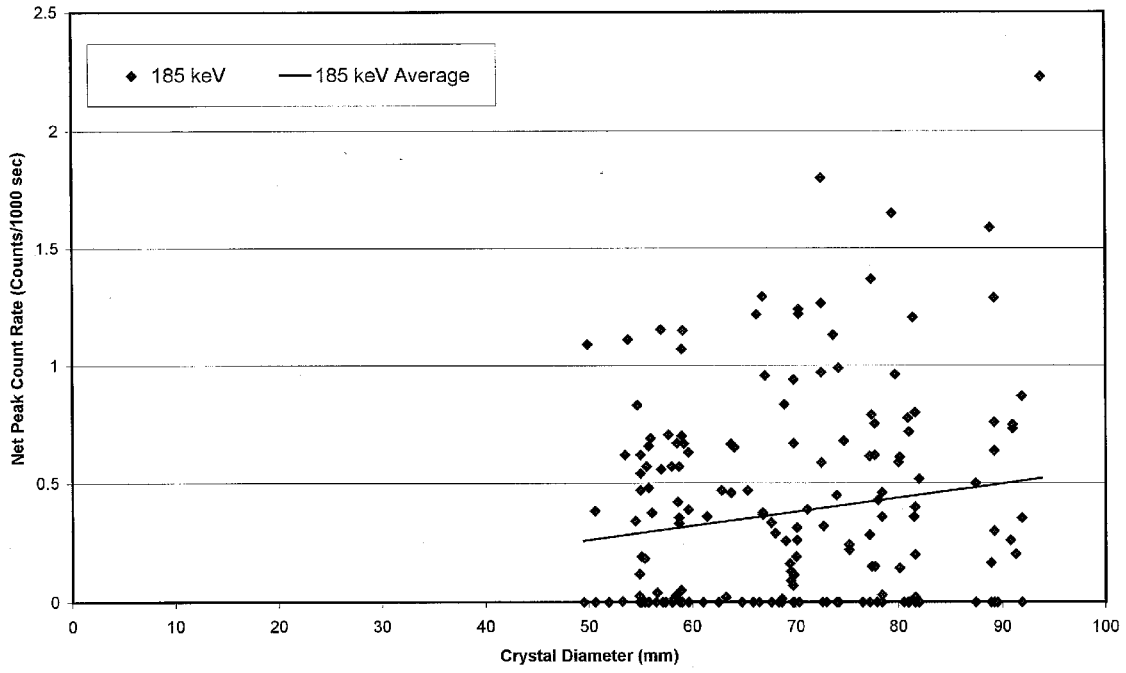


Figure 15

Net Peak Count Rate vs Length at 185 keV

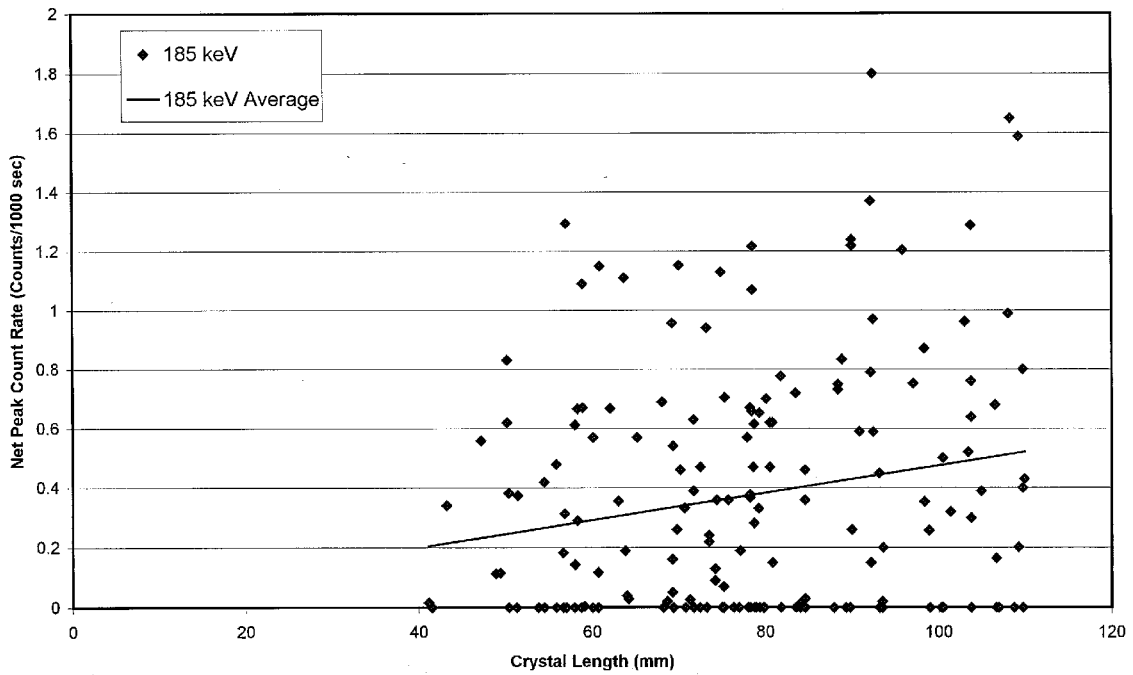
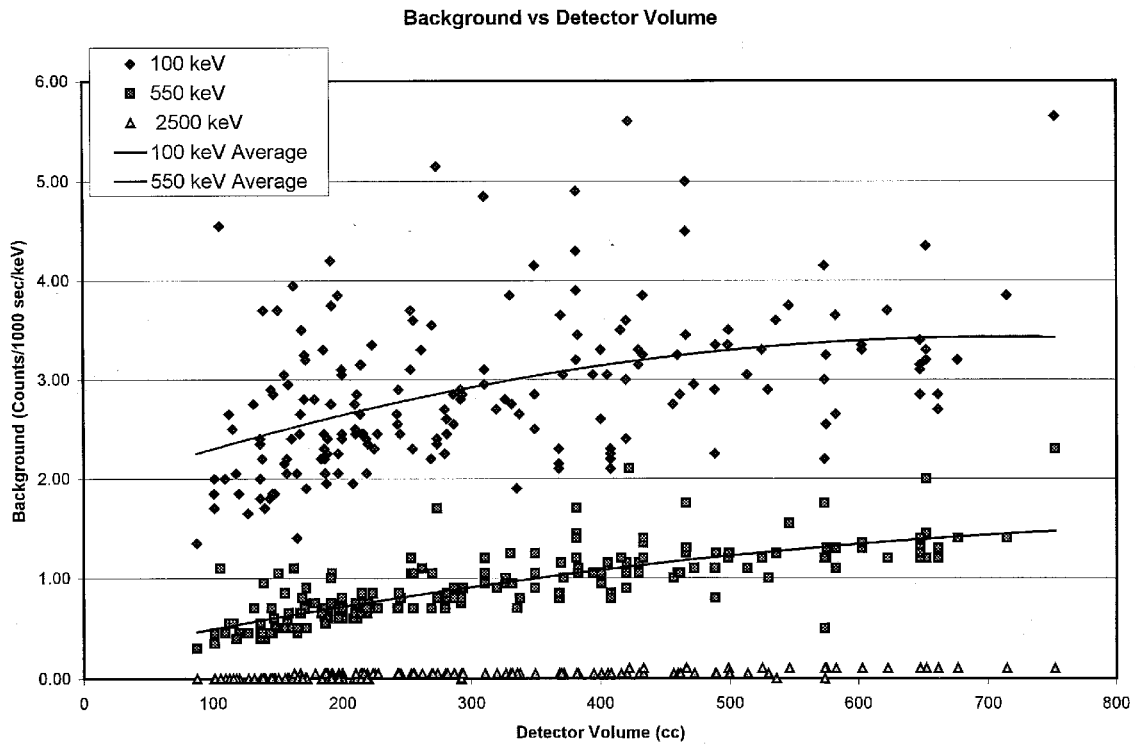
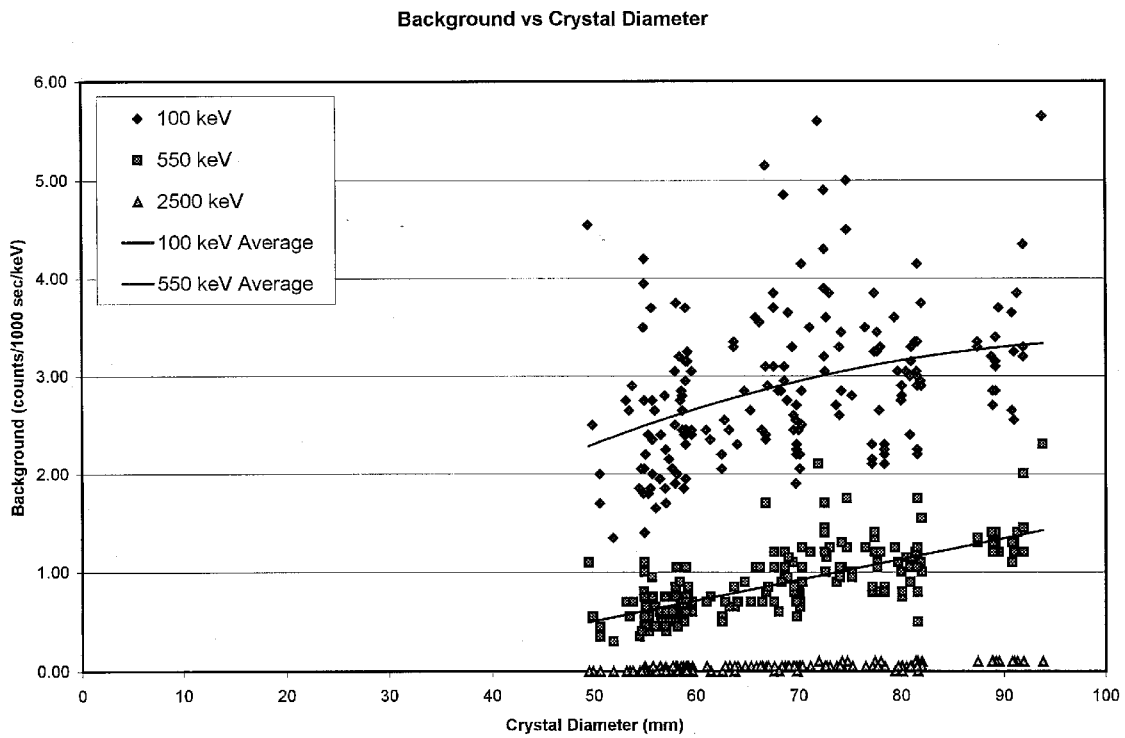


Figure 16



**Figure 17**



**Figure 18**

Background vs Crystal Length

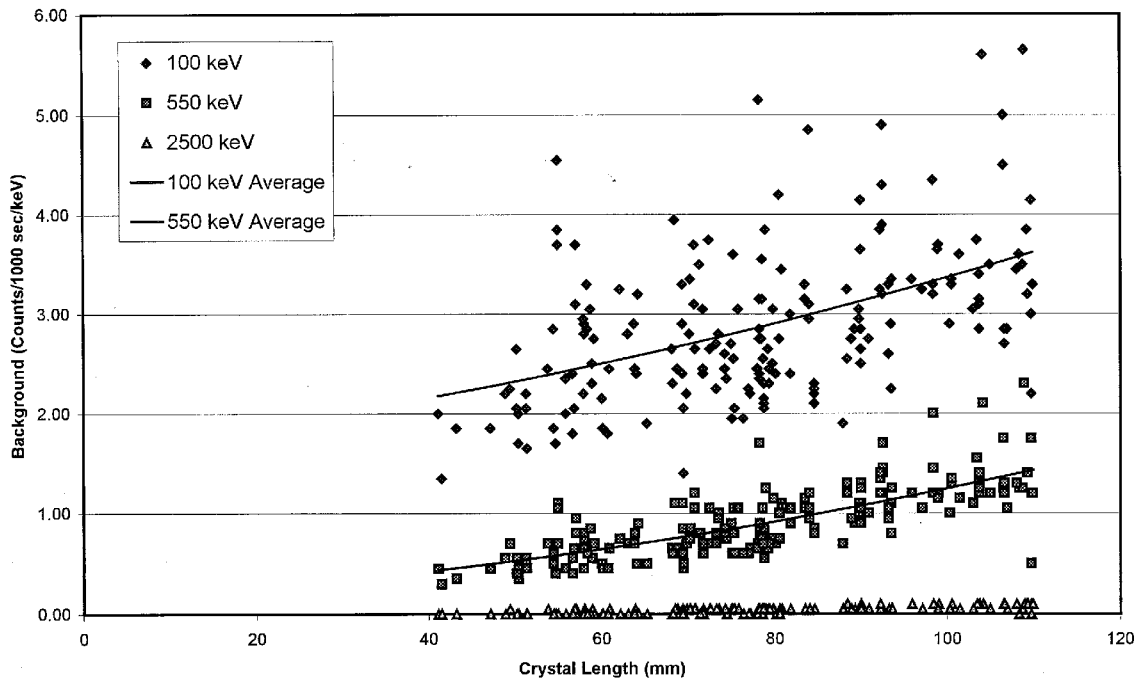


Figure 19

Background of 75 to 85 mm Diameter Crystals vs Length

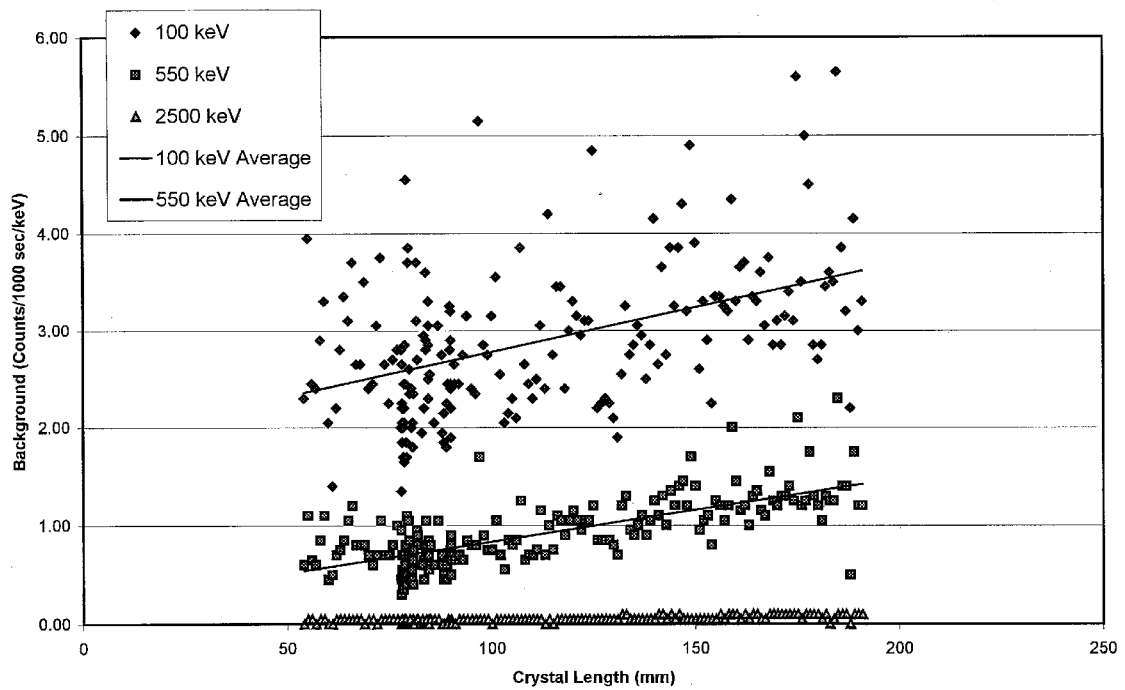


Figure 20

Background vs Length for 80 mm Diameter Crystals

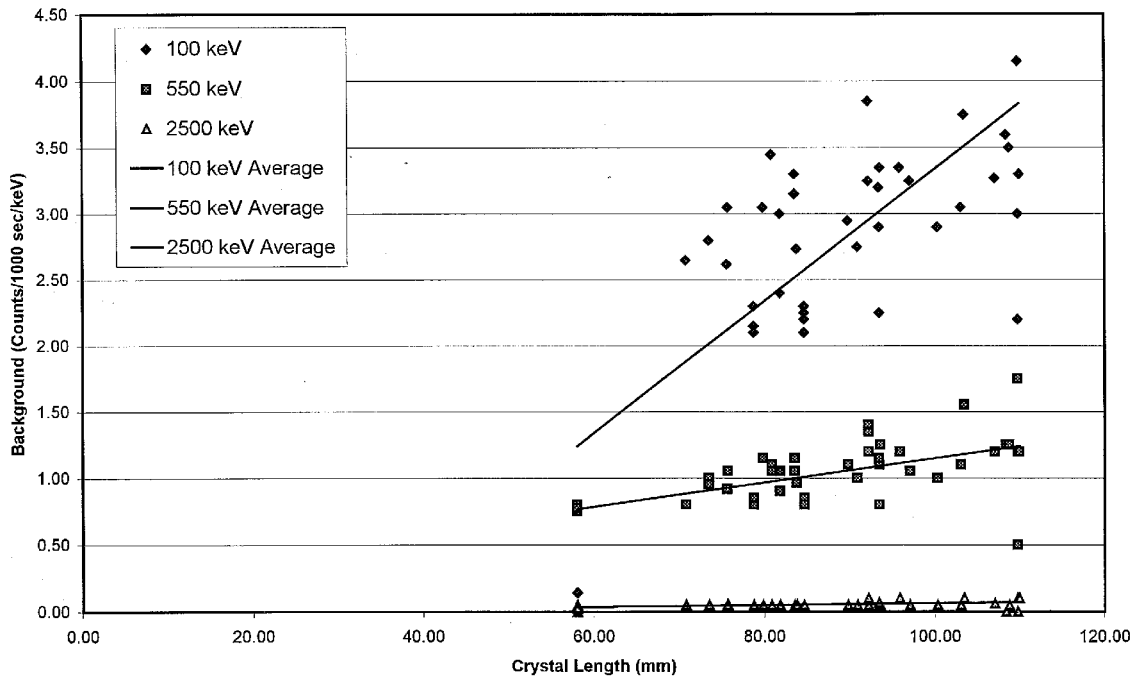


Figure 21

Relative MDA for 80 cm Diameter vs Length at 150 keV

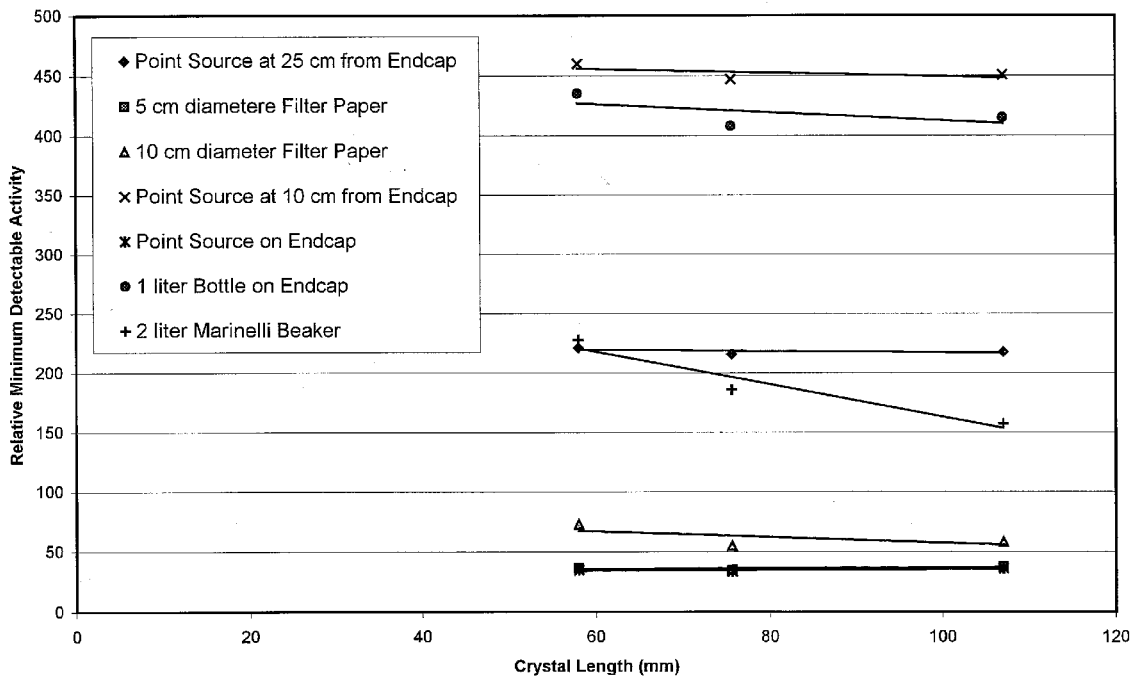


Figure 22

Relative MDA for 80 mm Diameter vs Length at 550 keV

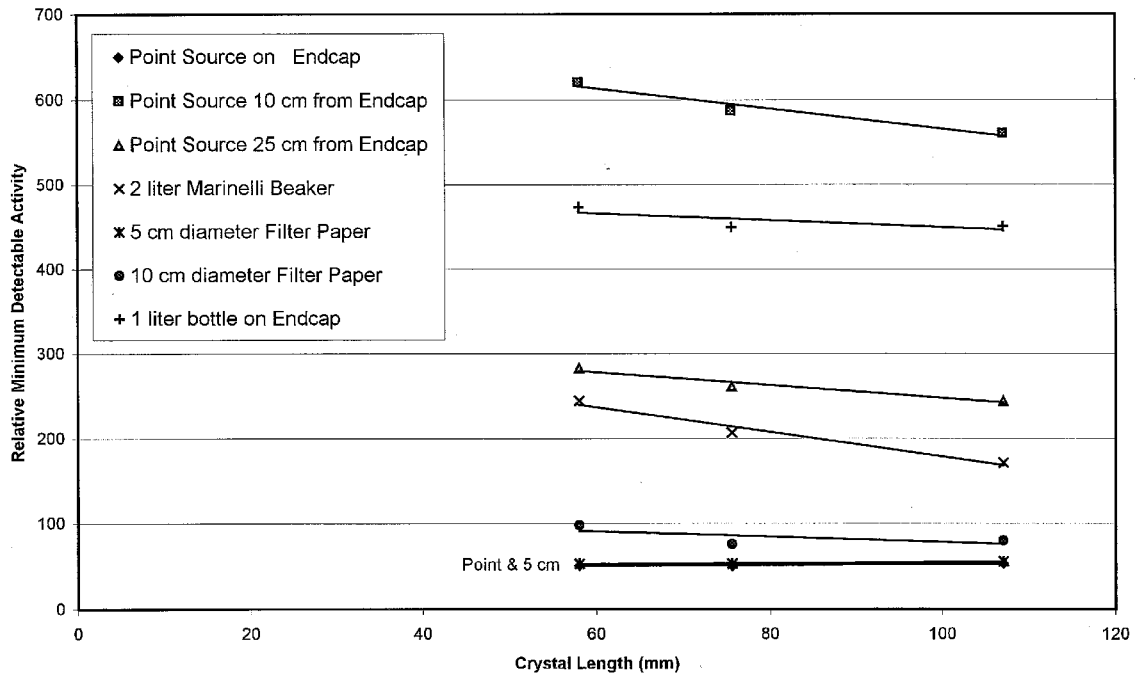


Figure 23

Relative MDA for 80 mm Diameter vs Length at 2500 keV

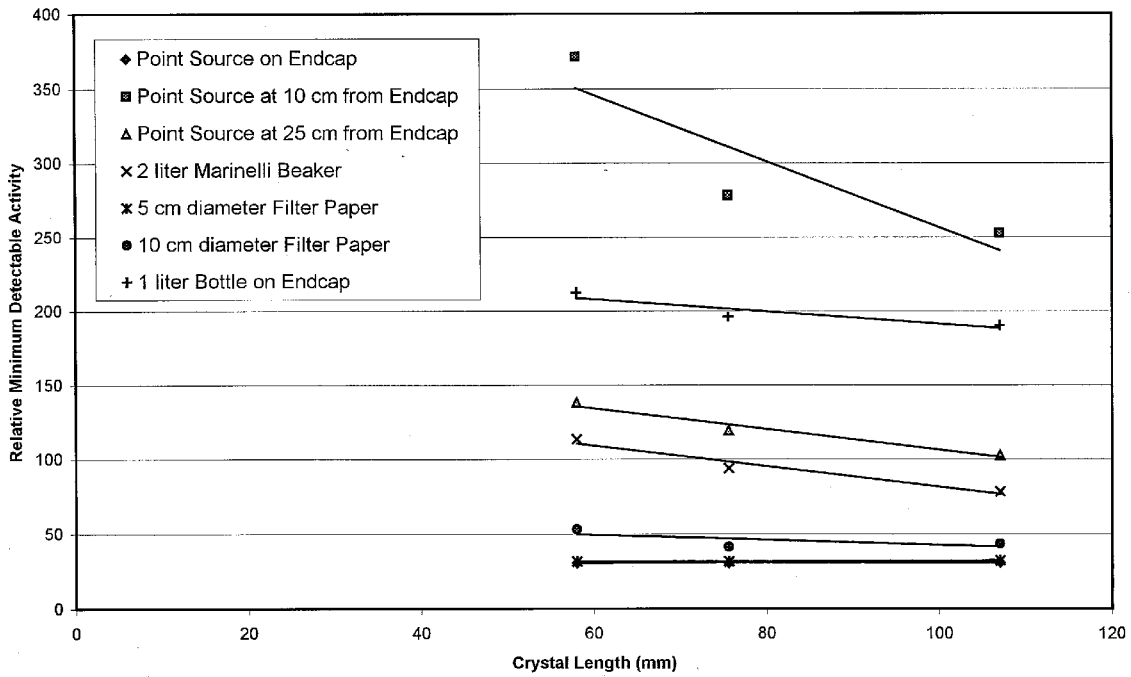
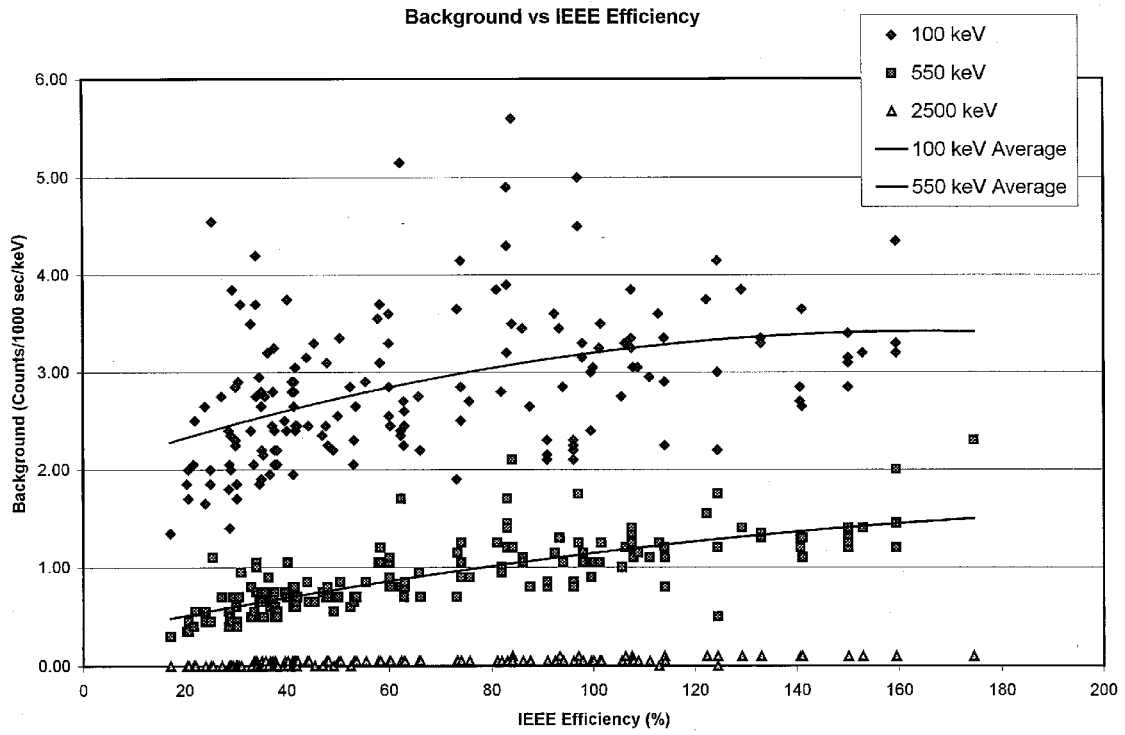


Figure 24



**Figure 25**